Estimation of Arbitrary Albedo and Shape from Shading for Symmetric Objects

Alper Yilmaz and Mubarak Shah
School of Computer Science
University of Central Florida
Orlando, FL-32828, USA
yilmaz,shah@cs.ucf.edu
http://www.cs.ucf.edu/∼vision

Abstract

In this paper, we propose a shape from shading (SFS) approach to recover both the shape and the reflectance properties of symmetric objects using a single image. The common constraint of constant or piece-wise constant albedo for lambertian surfaces is relaxed to arbitrary albedo. The proposed method can be categorized as a linear shape from shading method, which linearizes the reflectance function for symmetric objects using the symmetry cues of the shape and the albedo, and iteratively computes the depth values. Estimated depth values are then used to recover pixel-wise surface albedo. To show the usefulness of the proposed method, we present experimental results for both synthetic and real images.

1 Introduction

The problem of estimating shape of an object from its shading was first introduced by Horn [4]. He defined the mapping between the shading and the surface shape in terms of the reflectance function $I_{x,y} = R(p_{x,y}, q_{x,y})$ where $I_{x,y}$ is image intensity, $p = \frac{\partial z_{x,y}}{\partial x}$ and $q = \frac{\partial z_{x,y}}{\partial y}$, z being the height of the object and (x, y) are projected spatial coordinates of the 3D object. For simplicity, many researchers have used orthographic projection and Lambertian model for defining this mapping. Lambertian model is a diffuse reflectance model, where reflectance properties of a surface are defined in terms of the surface albedo and the angle between the surface normal and the light source direction. The standard reflectance function using Lambertian surface is given by

$$I_{x,y} = \rho_{x,y} \frac{1 + p_{x,y}P_s + q_{x,y}Q_s}{\sqrt{1 + p_{x,y}^2 + q_{x,y}^2}\sqrt{1 + P_s^2 + Q_s^2}} \tag{1}$$

where $P_s = \frac{\cos\tau \sin\sigma}{\cos\sigma}$, $Q_s = \frac{\sin\tau \sin\sigma}{\cos\sigma}$, τ is the tilt and σ is the slant of the illuminant. Once the mapping function is defined, recovering the shape ((p, q) or Z)

is a task of estimating the unknowns of the model which are the surface albedo ρ, and the surface gradients (p, q). With only the image intensities known and due to the nonlinear nature of the reflectance function, estimating both the depth and the albedo is ill-posed. For this reason, a common practice is to assume a constant surface albedo, which approximates surface as uniform region. However, for the real objects, uniform surface assumption is not correct, i.e. rendering the reconstructed shape with a different light source direction will not be realistic. In addition, it is concluded in a recent survey [14] that, due to simplistic model of constant albedo approximation, the depth estimates for real images are very poor.

There are mainly four different categories of SFS approaches: minimization, propagation, linearization and local methods. To overcome the short-coming of a constant albedo approximation different approaches apply different set of constraints. Minimization based methods use variational calculus to minimize an energy functional over the image, which is a combination of brightness and one or more of the following constraints: smoothness [5], integrability [3] and image gradient similarity [16]. A recent minimization based method proposed in [6] directly solves the shape by assuming the depth of the deepest surface point is known under constant albedo approximation. In contrast, propagation based methods propagate the known solution on the singular points [1] or the boundaries [4] to the whole surface. Local approaches assumes that any constraint imposed on the object (such as spherical approximation [10], etc) is valid only for the local patch, rather than the complete image. Linearization based approaches provides solution by linearizing the nonlinear reflectance function [11, 13]. A complete survey of most of these approaches can be found in [14].

The methods cited above try to solve the SFS problem by constraining the solution on the surfaces. Another possible approach is to constrain the type of objects. Recently, Shimshoni *et al.* [12] and Zhao and Chellappa [15] provided a shape from shading approach for symmetric objects. In [12], authors used geometric and photometric stereo to reconstruct 3D shape of quasi-frontal face images. In contrast, in [15] the authors used the symmetry constraints on depth and albedo to obtain another mapping function without the albedo term. The mutual solution of reflectance functions are then used to find the depth value of a point. However, both of these methods still constrain the albedo to be piece-wise constant, which is not realistic for the real surfaces that have arbitrary albedo fields.

Based on the definitions for symmetric surfaces, we propose a linear shape from shading algorithm for symmetric objects with arbitrary albedo field. Proposed method is based on linearizing the new symmetric reflectance function, which does not include the surface albedo information. We then use the linearized symmetric reflectance map to iteratively approximate the depth map $Z_{x,y}$ of the object. The recovered depth map is then used to estimate the albedo using (1).

The organization of the paper is as follows: in the next section, we will briefly describe the shape from shading and introduce the new reflectance function, which is based on the symmetry costraint. We will derive the iterative method for recovering the depth, which is followed by the discussion on obtaining the arbitrary albedo surface for the symmetric objects. In section 4, we will demonstrate experiments on synthetic and real images. Finally, conclusions are drawn.

2 SFS for Symmetric Objects

Uniqueness of the solution to the SFS problem is not possible without additional constraints, due to the number of unknowns and nonlinearity of the system. Obtaining a unique solution for SFS for constant albedo approximation was given in [8] by propagating the known solutions at singular points to the image. Similar results are also given in [2] for boundary conditions. However, in [14], it was shown that methods that guarantee unique solutions by propagation [1] are outperformed by minimization methods, which do not guarantee a unique solution. In this section, we will describe the symmetry constraint for defining an albedo free reflectance function.

2.1 Symmetry Constraint and New Reflectance Function

For the symmetric objects, the intensity on either side of the symmetry axis provides an additional constraint to obtain a unique solution for the SFS problem.

The definition of a symmetric surface given the symmetry axis can be expressed in terms of depth and albedo by $z_{x,y} = z_{-x,y}$ and $\rho_{x,y} = \rho_{-x,y}$. Note that the surface gradients are $p_{x,y} = -p_{-x,y}$ and $q_{x,y} = q_{-x,y}$. Due to the symmetry property the number of surface unknowns are halved compared to (1).Using symmetry definitions, the reflectance functions for either side of symmetry axis are

$$I_{x,y} = \rho \, \frac{1 + p_{x,y}P_s + q_{x,y}Q_s}{D} \qquad I_{-x,y} = \rho \, \frac{1 - p_{x,y}P_s + q_{x,y}Q_s}{D} \tag{2}$$

where $D = \sqrt{(1 + p_{x,y}^2 + q_{x,y}^2)(1 + P_s^2 + Q_s^2)}$. The ratio of $I_{x,y}$ and $I_{-x,y}$ in (2) provides a new reflectance function, which cancels the common albedo terms and the denominators. The new albedo free reflectance function is given by

$$r_{x,y}^I = \frac{I_{x,y} - I_{-x,y}}{I_{x,y} + I_{-x,y}} = \frac{p_{x,y}P_s}{1 + q_{x,y}Q_s} \tag{3}$$

Under the constant albedo approximation, (1) and (3) provide two equations in two unknowns p, q. Since (3) is linear, we can define p in terms of q. Substituting this back into (1) decreases number of unknowns to two, surface albedo (ρ) and one of the surface gradients (either p or q). In [15], Zhao and Chellappa approximated albedo, ρ, by piecewise constant values and solved the system for the other unknown. However, real objects do not exhibit constant albedo and the proposed method can not be generalized to arbitrary albedo estimation.

In the next section, we propose a linear algorithm for symmetric objects that estimates the depth by relaxing constant albedo to arbitrary albedo field.

3 Iterative Albedo Free Depth Calculation

The symmetry cue for the objects results in a generic albedo free reflectance function, which is given in (3). We treat symmetric reflectance function (3) as the only constraint that provides solution for unknows $Z_{x,y}$. Since a direct solution does not exist for (3), we developed an iterative scheme, which is detailed below.

Using the discrete approximations for the surface gradients, $p_{x,y} = Z_{x,y} - Z_{x-1,y}$ and $q_{x,y} = Z_{x,y} - Z_{x,y-1}$, we modify the reflectance function (3) as:

$$0 = f(r^I_{x,y}, Z_{x,y}, Z_{x-1,y}, Z_{x,y-1}) = r^I_{x,y} - \frac{P_s(Z_{x,y} - Z_{x-1,y})}{1 + Q_s(Z_{x,y} - Z_{x,y-1})}. \tag{4}$$

The solution for $Z_{x,y}$ in (4) depends on two other unknowns, $Z_{x-1,y}$ and $Z_{x,y-1}$. In order to find solution to these unknowns, we expand (4) into Taylor series about the points $\{Z^n_{x,y}, Z^n_{x-1,y}, Z^n_{x,y-1}\} = \{Z^{n-1}_{x,y} + \Delta Z_1, Z^{n-1}_{x-1,y} + \Delta Z_2, Z^{n-1}_{x,y-1} + \Delta Z_3\}$ and using only the first order terms, we obtain

$$0 = f_n \approx f_{n-1} + \Delta Z_1 \frac{\partial f_{n-1}}{\partial Z^{n-1}_{x,y}} + \Delta Z_2 \frac{\partial f_{n-1}}{\partial Z^{n-1}_{x-1,y}} + \Delta Z_3 \frac{\partial f_{n-1}}{\partial Z^{n-1}_{x,y-1}} \tag{5}$$

where

$$f_n = f(r^I_{x,y}, Z^n_{x,y}, Z^n_{x-1,y}, Z^n_{x,y-1}) \qquad f_{n-1} = f(r^I_{x,y}, Z^{n-1}_{x,y}, Z^{n-1}_{x-1,y}, Z^{n-1}_{x,y-1}) \tag{6}$$

Eq. (5) can be simplified by letting constants $(\Delta Z_2, \Delta Z_3) = (0, 0)$. Using the definitions from (4) iterative depth update can be derived from (5) simply:

$$Z^n_{x,y} = Z^{n-1}_{x,y} - \epsilon = Z^{n-1}_{x,y} - \frac{r^I_{x,y} - \frac{P_s(Z^{n-1}_{x,y} - Z^{n-1}_{x-1,y})}{1+Q_s(Z^{n-1}_{x,y} - Z^{n-1}_{x,y-1})}}{\frac{\partial f^{n-1}}{\partial Z^{n-1}_{x,y}}} \tag{7}$$

After some algebraic manipulations, the gradient term $\frac{\partial f^{n-1}}{\partial Z^{n-1}_{x,y}}$ becomes

$$\frac{\partial f^{n-1}}{\partial Z^{n-1}_{x,y}} = - \frac{P_s \ \left(1 + Q_s(Z^{n-1}_{x-1,y} - Z^{n-1}_{x,y-1})\right)}{\left(1 + Q_s(Z^{n-1}_{x,y} - Z^{n-1}_{x,y-1})\right)^2} \tag{8}$$

Substituting (4) and (8) into (7) the final iterative equation for depth is given by

$$Z^n_{x,y} = Z^{n-1}_{x,y} + \frac{r^I_{x,y} \ \beta^2_{x,y} - P_s \ \beta_{x,y} \ (Z^{n-1}_{x,y} - Z^{n-1}_{x-1,y})}{P_s \ \beta_{x,y} - P_s \ Q_s \ (Z^{n-1}_{x,y} - Z^{n-1}_{x-1,y})} \tag{9}$$

where $\beta_{x,y} = 1 + Q_s \ (Z^{n-1}_{x,y} - Z^{n-1}_{x,y-1})$.

3.1 Estimating Arbitrary Albedo for Symmetric Objects

For estimating the shape of an object, a common practice is to use constant albedo for the image. An extension to this is to use piece-wise constant albedo, where the albedo is relaxed to have different values for different segments of the image. For the latter approach, Zheng and Chellappa [16] assume surface patches to be locally flat and the surface normal tilt and slant to be independent of each other. In contrast, Lee and Rosenfeld [7] assume the surface patches to be locally spherical and use a Gaussian sphere to derive the probability density function of the surface normal tilt and slant. Based on these assumptions both methods first solve the slant of the light source, which is followed by estimating the albedo. However,

due to the constraints imposed on the surface, they fail on the boundary regions. Besides, for real objects the surface assumptions is not necessarily true.

Our proposed approach for albedo estimation is a direct application of standard reflectance function given in (1). After recovering the depth values using the proposed method described in Sect. 3, we substitute them back in (1) and evaluate

$$\rho_{x,y} = I_{x,y} \frac{\sqrt{1+(z_{x,y}-z_{x-1,y})^2+(z_{x,y}-z_{x,y-1})^2}\sqrt{1+P_s^2+Q_s^2}}{1+P_s(z_{x,y}-z_{x-1,y})+Q_s(z_{x,y}-z_{x,y-1})} \tag{10}$$

to obtain pixel based arbitrary albedo values $\rho_{x,y}$.

For clarification of the proposed method, it should be noted that, in contrast to [15], the depth estimates are found solely using the symmetric reflectance function (4), which relaxes the albedo term in (1) to be arbitrary for symmetric objects.

4 Experiments

To illustrate the performance of the proposed depth recovery and albedo estimation method, we first tested the algorithms on synthetic images, which include laser range image of Mozart statue (Fig. 1a) synthetic images of sphere (Fig. 2a) and vase (Fig. 3a). The experiments on synthetic images are performed for constant and varying albedo surfaces. For recovering the depth, we only used symmetric regions of the images by masking out the non-symmetric regions and initial depth for the iterations is set to $Z_0 = 0$. The proposed method is also tested using a number of real frontal face images, since the ground truth for the light source directions are not known, we used the light source direction estimation method proposed by Pentland [9].

We evaluated the performance of the methods for depth and albedo surface estimation both qualitatively and quantitatively. For qualitative analysis, 3D plots of the estimated depth maps and albedo surfaces are generated. Specifically for Mozart, we generated images under different light source directions with constant albedo ($\rho = 1$). Figures in first column of 1b,c and d show the generated images under different lighting conditions from the Mozart range map. Corresponding recovered depth maps and the albedo surface are given in second and third columns respectively. Note that due to symmetry constraint we only used the face region of the original Mozart range map. As can be observed from the recovered depth map of the Mozart given in Figure 1, the nose is inset due to similar $r^I_{x,y}$ values around the nose region and the cheek region.

For real face images, we initialized the depth both by $Z_{x,y} = 0$. For the face image shown in Fig. 4a, the method converged in thirteen iterations. Recovered depth for each iteration is shown in Fig. 4e. In Fig(s). 4c and d, we illuminated the face image using different light sources using the recovered depth map and the albedo (Fig. 4b).

We also tested the method for synthetic surfaces that have complex varying albedo surfaces. As shown in Fig. 2b, the albedo surface for the sphere object is generated using a cosine wave; corresponding 3D plots of the recovered depth maps and albedo surface for the sphere image in Fig. 2c are given in Fig(s). 2d and e respectively. Similarly, for the vase object, the albedo surface is generated

Table 1: Mean and standard deviation of error in depth Z, and mean of surface gradients $\frac{\partial Z}{\partial x}$, $\frac{\partial Z}{\partial y}$ errors.

	albedo surface	**light source** (s_x, s_y, s_z)	**Depth mean error**	**Depth stdv. error**	**Gradient mean err.**
Mozart	constant	$(-.3, .5, 1)$	3.55	4.54	1.20
Sphere	variable	$(-.6, 0, 1)$	5.2	8.9	0.28
Vase	variable	$(-.6, .2, 1)$	3.02	4.01	0.74

Table 2: Mean and standard deviation of errors in albedo ρ.

	albedo surface	**light source** (s_x, s_y, s_z)	**Albedo mean error**	**Albedo stdv. error**
Mozart	constant	$(-.3, .5, 1)$	0.02	0.06
Sphere	variable	$(-.6, 0, 1)$	0.1	0.2
Vase	variable	$(-.6, .2, 1)$	0.29	0.2

using combination of sine and cosine waves (Fig. 3b). Recovered depth and albedo surfaces for the vase image of Fig. 3c are shown in Fig(s). 3d and e respectively. Note that for both of these examples current schemes can not recover the correct depth maps and albedo surfaces.

For quantitative analysis, in order to be consistent with the comparison given in survey paper on SFS [14], we tabulated the mean and standard deviation of the depth error and mean gradient error in Table 1. In addition, mean and standard deviation of the albedo error are tabulated in Table 2. The depth errors are obtained from the true depth map and the normalized recovered depth map. The range of the depth values used to construct Table 1 are $0 < Z < 38$ for the vase, $0 < Z < 34$ for the Mozart and $0 < Z < 30$ for the sphere. Similarly albedo errors given in Table 2 are calculated from the ground truth and the estimated albedo values. The range for the albedo values for all objects are $0 < \rho < 1$. The quantitative analysis are not performed for the real images due to the lack of ground truth for the depth. The CPU timing of the proposed method is 0.5 sec(s) for a 128x128 symmetric image for 6 iterations.

5 Conclusion

We propose a two step algorithm to recover shape and reflectance properties for symmetric objects. The symmetry constraints are used to obtain a new albedo free reflectance function. The method uses Taylor series expansion of the symmetric reflectance function to iteratively calculate the depth value at a pixel. The depth value at each pixel is dependent only on the light source direction, intensity at pixels on either side of the symmetry axis and the two neighboring depth values.

After the depth values are obtained, the standard reflectance function is used to recover the pixel based albedo values, which relaxes the constant albedo approximation. Experiments on synthetic and real images show the usefulness of the proposed approach for recovering both the shape and the albedo of the object.

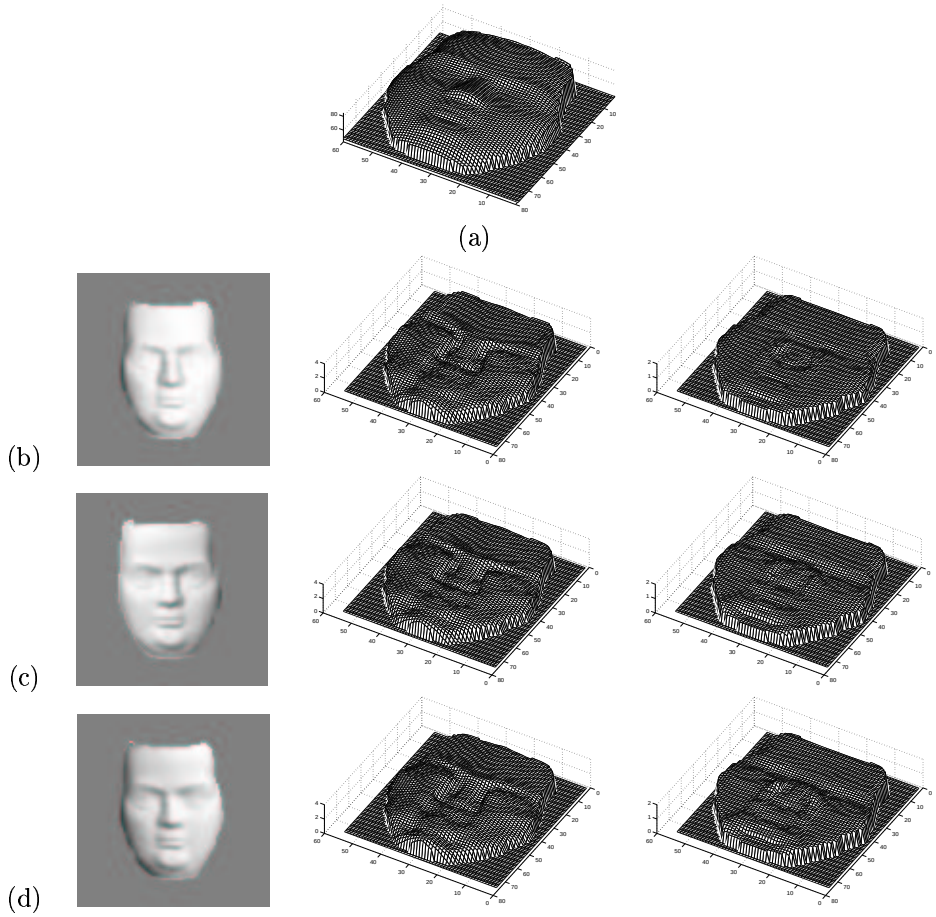

Figure 1: (a) Original Mozart depth map; first column input images, second column recovered depth maps, third column estimated albedo surfaces for light source (s_x, s_y, s_z) at (b) $= (0.2, 0.1, 1)$, (c) $(-0.3, 0.5, 1)$ and (d) $(0.5, 0.5, 1)$

References

[1] M. Bichel and A. Pentland. A simple algorithm for shape from shading. In *IEEE Conf. CVPR*, pages 459–465, 1992.

[2] A. Blake and A. Zisserman. Surface descriptions from stereo and shading. *Image and Vision Computing Journal*, 3(2):183–191, 1992.

[3] R.T. Frankot and R. Chellappa. A method for enforcing interability in shape from shading algorithms. *IEEE Trans. on PAMI*, 10:439–451, 1988.

[4] B.K.P. Horn. *Shape from Shading: A method for Obtaining the Shape of a Smooth Opaque Object from One View.* PhD Thesis, MIT, 1970.

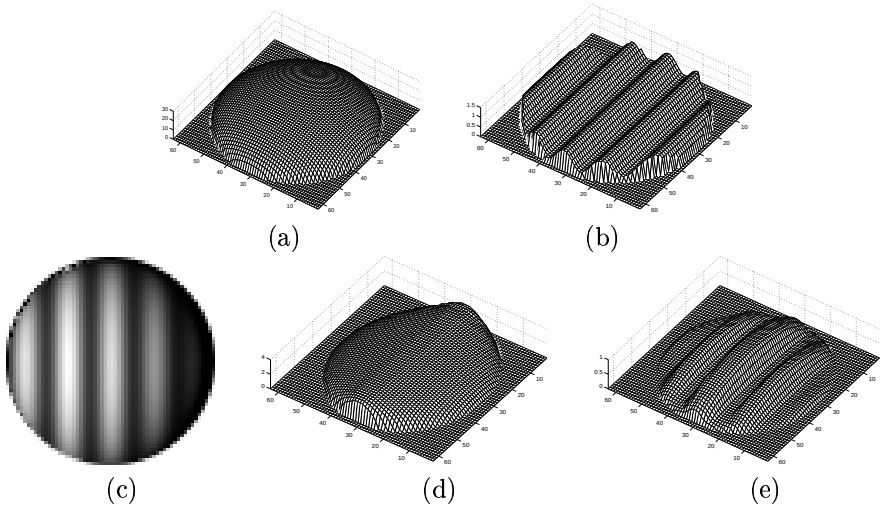

Figure 2: Original depth map (a), albedo surface(b); (c)image generated with light source $(s_x, s_y, s_z) = (-.6, 0, 1)$, recovered depth map (d); estimated albedo (e).

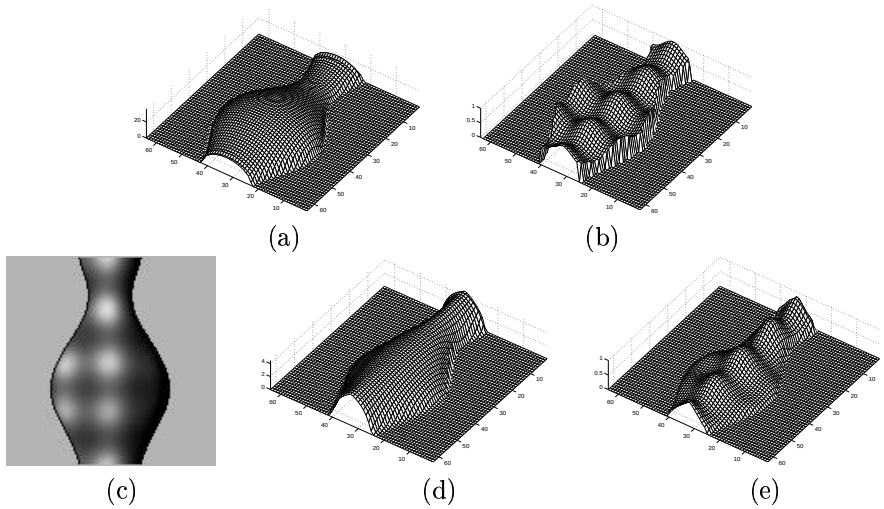

Figure 3: Original depth map (a), albedo surface(b); (c)image generated with light source $(s_x, s_y, s_z) = (-.6, .2, 1)$, recovered depth map (d); estimated albedo (e).

[5] K. Ikeuchi and B.K.P. Horn. Numerical shape from shading and occluding boundaries. *Artificial Intelligence*, 17(1-3):141–184, 1981.

[6] R. Kimmel and J.A. Sethian. Optimal algorithm for shape from shading and path planning. *JMIV Journal*, 14(3):237–244, 2001.

[7] K.M. Lee and A. Rosenfeld. Albedo estimation for scene segmentation. *Pattern Recognition Letters*, 1:155–160, 1983.

[8] J. Oliensis. Uniqueness in shape from shading. *IJCV Journal*, 6:75–104, 1991.

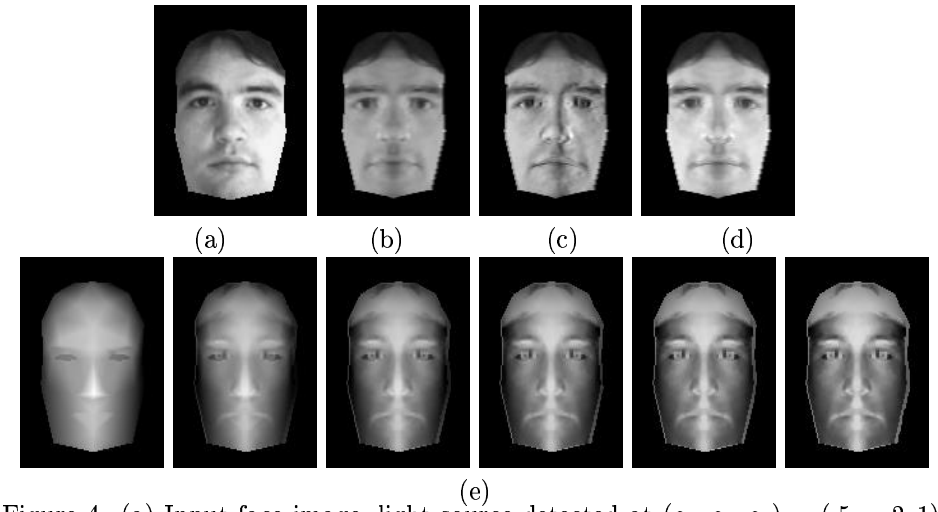

Figure 4: (a) Input face image, light source detected at $(s_x, s_y, s_z) = (.5, -.2, 1)$; (b) recovered albedo; synthesized image light source at (c) $(s_x, s_y, s_z) = (-.8, 0, 1)$, (d) $(s_x, s_y, s_z) = (0, 0, 1)$; (e) recovered depth for selected iterations.

[9] A. Pentland. Finding the illuminant direction. *Journal of Optical Society of America*, pages 448–455, 1982.

[10] A. Pentland. Local shading analysis. *IEEE Trans. on PAMI*, 6:170–187, 1984.

[11] A. Pentland. Shape information from shading: A theory about human perception. In *IEEE Conf. ICCV*, pages 404–413, 1988.

[12] I. Shimshoni, Y. Moses, and M. Lindenbaum. Shape reconstruction of 3d bilaterally symmetric surfaces. *IJCV Journal*, 39(2):97–110, 2000.

[13] P.S. Tsai and M. Shah. Shape from shading using linear representation approximation. *Image and Vision Computing Journal*, 12(8):487–498, 1994.

[14] R. Zhang, P.S. Tsai, J.E. Cryer, and M. Shah. Shape from shading: A survey. *IEEE Trans. on PAMI*, 21(8):690–706, 1999.

[15] W. Zhao and R. Chellappa. Illumination insensitive face recognition using symmetric shape from shading. In *IEEE Conf. CVPR*, pages 286–293, 2000.

[16] Q. Zheng and R. Chellappa. Estimation of illuminant direction, albedo and shape from shading. *IEEE Trans. on PAMI*, 13(7):680–702, 1991.